Accepted Preprint first posted on 25 August 2016 as Manuscript EJE-16-0639

Successful treatment of residual pituitary adenoma in persistent acromegaly following localisation by ^{11}C-methionine PET-CT co-registered with MRI

Olympia Koulouri[1], Narayanan Kandasamy[1], Andrew C Hoole[2], Daniel Gillett[3], Sarah Heard[3], Andrew S Powlson[1], Dominic G O'Donovan[4], Anand K Annamalai[1], Helen L Simpson[1], Scott A Akker[10], Simon JB Aylwin[11], Antonia Brooke[12], Harit Buch[13], Miles J Levy[14], Niahm Martin[15], Damian Morris[16], Craig Parkinson[16], James R Tysome[5], Tom Santarius[6], Neil Donnelly[5], John Buscombe[3], Istvan Boros[9], Rob Smith[9], Franklin Aigbirhio[9], Nagui M Antoun[7], Neil G Burnet[8], Heok Cheow[3], Richard J Mannion[6], John D Pickard[6,9], Mark Gurnell[1]

[1]Metabolic Research Laboratories, Institute of Metabolic Science, and [2]Departments of Medical Physics, [3]Nuclear Medicine, [4]Pathology, [5]Otolaryngology, [6]Neurosurgery, [7]Neuroradiology, [8]Radiation Oncology and the [9]Wolfson Brain Imaging Centre, University of Cambridge and National Institute for Health Research Cambridge Biomedical Research Centre, Addenbrooke's Hospital, Cambridge, UK.

[10]Department of Endocrinology, St Bartholomew's Hospital, London, UK; [11]Department of Endocrinology, King's College Hospital, London, UK; [12]Macleod Diabetes and Endocrine Centre, Royal Devon and Exeter Hospital, Exeter, UK; [13]Department of Diabetes and Endocrinology, New Cross Hospital, Wolverhampton, UK; [14]Department of Endocrinology, Leicester Royal Infirmary, Leicester, UK; [15]Department of Endocrinology, Imperial College Healthcare NHS Trust, London, UK; [16]Diabetes and Endocrine Centre, Ipswich Hospital, Ipswich, UK.

Corresponding author: Dr M Gurnell, Metabolic Research Laboratories, Institute of Metabolic Science, University of Cambridge, Box 289, Addenbrooke's Hospital, Hills Road, Cambridge, CB2 0QQ, UK; Tel:+44-1223-348739; Fax:+44-1223-330598; E-mail: mg299@medschl.cam.ac.uk

Abbreviated title: MetPET/MRI in persistent acromegaly

Key words: ^{11}C-Methionine PET-CT, SPGR MRI, co-registration, acromegaly, pituitary

Word Count: Abstract 250; text 3437; table 1; figures 7.

Copyright © 2016 European Society of Endocrinology.

Abstract

Objective: To determine if functional imaging using ^{11}C-methionine positron emission tomography computed tomography, co-registered with 3D gradient echo MRI (Met-PET/MRI), can identify sites of residual active tumour in treated acromegaly, and discriminate these from post-treatment change, to allow further targeted treatment.

Design/Methods: Twenty-six patients with persistent acromegaly following previous treatment, in whom MRI appearances were considered indeterminate, were referred to our centre for further evaluation over a 4.5-year period. Met-PET/MRI was performed in each case and findings were used to inform decision-making regarding adjunctive therapy. Four patients with clinical and biochemical remission post-transsphenoidal surgery (TSS), but in whom residual tumour was suspected on postoperative MRI, were also studied.

Results: Met-PET/MRI demonstrated tracer uptake only within the normal gland in the four patients who had achieved complete remission following primary surgery. In contrast, in 26 patients with active acromegaly, Met-PET/MRI localised sites of abnormal tracer uptake in all but one case. Based on these findings, fourteen subjects underwent endoscopic TSS, leading to a marked improvement in (n=7), or complete resolution of (n=7), residual acromegaly. One patient received stereotactic radiosurgery and two patients with cavernous sinus invasion were treated with image-guided fractionated radiotherapy, with good disease control. Three subjects await further intervention. Five patients chose to receive adjunctive medical therapy. Only one patient developed additional pituitary deficits following Met-PET/MRI-guided TSS.

Conclusions: In patients with persistent acromegaly following primary therapy, Met-PET/MRI can help identify the site(s) of residual pituitary adenoma when MRI appearances are inconclusive, and direct further targeted intervention (surgery or radiotherapy).

Introduction

Transsphenoidal surgery (TSS) remains the treatment of choice for functioning pituitary tumours causing acromegaly, Cushing's disease and central hyperthyroidism (thyrotropinoma), and in patients with prolactinoma who are intolerant of medical therapy. However, even in experienced hands persistent/recurrent disease requiring additional therapy (repeat surgery, radiotherapy or long-term medical treatment) is not uncommon, and in the case of acromegaly may be required in up to 50% of macroadenomas (1). Postoperative decision-making in these patients is guided by several factors, including clinical and biochemical assessment of endocrine status and the identification of residual tumour on follow-up scanning. However, standard pituitary imaging [magnetic resonance imaging (MRI) or, less commonly, computerised tomography (CT)] does not always reliably distinguish between residual tumour, post-surgical change and normal pituitary tissue (2, 3). In this context, the likelihood that the patient will be offered further treatment with targeted therapies such as repeat TSS or stereotactic radiosurgery is diminished. Although conventional fractionated radiotherapy is effective in controlling residual endocrine hyperfunction and preventing tumour growth, it carries an increased risk of hypopituitarism (4). In addition, potential links to second tumour growth (e.g. meningioma) and premature cerebrovascular disease have also been suggested (5), although recent studies have shown no additional excess beyond that observed in patients undergoing surgery alone (6, 7).

More reliable techniques for discriminating between residual functioning tumour, post-treatment change and the normal pituitary gland could therefore help identify those patients with persisting acromegaly who are most likely to benefit from repeat TSS or targeted radiotherapy. A role for functional imaging in the post-operative management of pituitary tumours has been proposed previously, but is not currently in routine clinical use (2, 3, 8, 9). ^{18}F-fluorodeoxyglucose (FDG), the positron emission tomography (PET) tracer most commonly employed in oncology, has been used successfully to locate microadenomas or residual tumour following surgery in some patients but, importantly, it lacks sensitivity and its utility is also limited by high uptake into surrounding normal brain tissue (8, 9). In contrast, ^{11}C-methionine exhibits a more favourable pituitary to brain uptake

ratio, and several studies have demonstrated its ability to identify residual pituitary adenoma (2, 3, 9, 11). However, a key limitation in many of the early studies was the restricted anatomical resolution offered by PET or PET-CT. This presents a particular challenge when trying to accurately localise small (sub-centimeter) lesions, which may not be readily differentiated from uptake into adjacent normal pituitary tissue (12). The absence of readily-available PET-MRI has prompted some workers to assess the utility of merging (co-registering) PET-CT and MRI images (Met-PET/MRI) to provide enhanced anatomical definition at sites of ^{11}C-methionine tracer uptake (9, 10). However, to date little data correlating imaging findings with subsequent treatment decisions and clinical outcomes has been reported (9, 10).

Here, we report our findings in 30 consecutive patients with acromegaly referred to our service for further evaluation because of indeterminate post-treatment MRI appearances, and describe how treatment decisions were informed by the findings on Met-PET/MRI.

Subjects and Methods

Patients

Between June 2011 and December 2015, 30 patients [16 women, 14 men; mean age 48 yr (range 24-75 yr)] were referred to our university teaching hospital pituitary service for further evaluation of suspected or confirmed residual active acromegaly following primary therapy [TSS alone in 23 patients; TSS with adjunctive fractionated radiotherapy (RT) in three patients; TSS with adjunctive RT and stereotactic radiosurgery (SRS) in one patient; and primary medical therapy in three patients (lanreotide Autogel®, n=1; cabergoline, n=1; pegvisomant, n=1)] (Table 1). In all cases of active disease, patients exhibited typical clinical features, with elevated insulin-like growth factor 1 (IGF-1, above the age and sex-matched reference range), and failure to suppress serum growth hormone (GH) to <0.4 mcg/L after a 75 g oral glucose load, and/or GH levels >2.5 mcg/L (either random measurement or mean of five samples drawn at 30-60 minute intervals) (13). Post-treatment imaging had been deemed indeterminate following review by a specialist pituitary multidisciplinary team (see below) in the referring centre. For patients receiving adjunctive medical therapy at the point of referral, we advised discontinuation of depot SSA therapy for a minimum of 12 weeks, and dopamine agonist therapy for 4 weeks, prior to Met-PET/MRI.

Biochemical measurements

All analytes were measured by a Clinical Pathology Accreditation Limited laboratory (CPA, Middlesex, UK) with relevant internal and external quality assurance as defined by the CPA. Serum GH concentration was measured using a solid phase two-site time-resolved fluorometric assay (DELFIA®, PerkinElmer Life and Analytical Sciences Inc., Waltham, Massachusetts, USA) calibrated to IS 98/574 (analytical sensitivity 0.01 ng/mL; interassay coefficient of variation <5 % across the range 0.025–25 ng/mL). Serum samples giving GH higher than this were diluted with zero standard as provided by the manufacturer. Serum IGF-1 was measured using a solid-phase enzyme labelled chemiluminescent immunometric assay (Siemens Immulite2000® – Siemens Medical Solutions Diagnostics Ltd., Llanberis, Gwynedd, UK) calibrated to IS 87/518 (analytical sensitivity 20 ng/mL;

interassay coefficient of variation <10 % across the range 25–1600 ng/mL), and results are shown as × upper limit of normal (×ULN).

Clinical care

All patients were managed in accordance with local and international clinical guidelines (14) and all patients provided informed consent for Met-PET-CT and 3D gradient echo MRI. The decision to offer further treatment was undertaken on a case-by-case basis following discussion by a specialist pituitary multidisciplinary team (MDT) comprising pituitary neurosurgeon(s), endocrinologist(s), otolaryngologist(s), radiation oncologist(s), neuropathologist(s) and neuroradiologist(s), who had full access to the Met-PET/MRI scans to aid decision-making. Further surgery or radiotherapy was undertaken either at our centre or the referring hospital. The study received Institutional approval.

Pathological examination

Surgical specimens were fixed in 10% neutral buffered formalin and embedded in paraffin. Histopathological confirmation of the presence of a somatotroph tumour was verified by the findings of typical microscopic appearances for a pituitary adenoma with positive immunohistochemical (IHC) staining for growth hormone.

Synthesis of ^{11}C-methionine

The PET tracer, L-[methyl-^{11}C]-methionine, was synthesised in compliance with good manufacturing practice using a captive solvent in loop methylation method without preparative HPLC, adapted from methods published previously (15-17). Briefly, [^{11}C]CO2 was produced using a PETtrace cyclotron (GE Medical Systems) via the ^{14}N(p,α)^{11}C reaction before conversion to [^{11}C]MeI in the MeI MicroLab (GE Medical Systems). This was then transferred to the HPLC loop of a modified TracerLabFXC (GE Medical Systems) synthesiser containing an L-homocysteine precursor solution (0.5M aqueous NaOH solution in ethanol). ^{11}C-methionine was produced in yields up to 15GBq with a

radiochemical purity of >96% and specific activity between 32.2 and 1564 GBq/μmol (average 205.5 GBq/μmol).

Met-PET imaging

All scans were acquired on a GE Discovery 690 PET-CT scanner (GE Medical Systems, Milwaukee, WI, USA). The study was performed 20 min after intravenous administration of 300-400 MBq of L-[methyl-^{11}C]- methionine. A low dose CT (140 kV, 220 mA, 0.5s rotation, 0.984 mm pitch) was acquired for attenuation correction followed by a single bed position PET study of the head. Time-of-Flight (ToF) PET data were acquired for a total acquisition time of 20 min. PET images were reconstructed with CT attenuation correction using fully 3D iterative reconstruction algorithms (3 iterations, 24 subsets, 2 mm Gaussian post-filter) incorporating ToF & resolution recovery software (VUE Point FX and Sharp IR) to a 3.27 mm slice thickness. The CT images were reconstructed at 1.25 mm slice thickness. Met-PET studies were reviewed by nuclear medicine physicians with expertise in PET-CT on the Xeleris workstation (GE Healthcare).

Standard and 3D gradient echo MRI

Imaging was performed on a 1.5T superconducting unit (GE Signa®, Milwaukee, USA) using a circularly-polarised head coil. For standard clinical MRI, coronal T1-weighted spin echo images were obtained before and after intravenous injection of 0.1 mmol/kg gadopentetate dimeglumine. Subsequently, a spoiled gradient recalled acquisition (SPGR) sequence was also performed to optimise co-registration with the Met-PET dataset. In brief, sagittal T1-weighted fast spoiled gradient echo images (TR 11.5 ms, TE 4.2 ms, slice thickness 1 mm, 0 mm gap, 256 × 256 matrix) of the whole head were obtained. The absence or presence of cavernous sinus invasion was defined according to Knosp criteria (18). MRI scans were reviewed by neuroradiologists and members of the pituitary MDT both at the local/referring hospitals and in Cambridge.

Co-registration of Met-PET and MRI

Met-PET and MRI images were co-registered using ProSoma version 3.3, Build 252 software (MedCom GmbH). ProSoma is a virtual simulation package used primarily in radiotherapy. It allows multiple datasets to be loaded simultaneously and co-registered with each other using a mutual information based automatic registration algorithm. For the purposes of this work the SPGR MRI sequence was selected as the primary dataset. The CT dataset acquired as part of the Met-PET imaging was then registered to the MRI and the resulting registration parameters applied to the PET data to achieve a Met-PET/MRI registration.

Results

Patients with indeterminate MRI appearances but complete remission of acromegaly

Four patients (cases 1–4) were in complete remission (clinically and biochemically) following primary TSS (Table 1). However, in each of these patients the post-operative MRI (performed at 3-4 months after surgery) showed suspected residual disease at the site of the original tumour. Two neuroradiologists were unable to distinguish between possible residual tumour and post-operative change in each of these patients. In contrast, Met-PET/MRI showed only tracer accumulation corresponding to the normal pituitary gland, with no uptake at sites of suspected residual tumour (Figs 1 and 2).

Patients with indeterminate MRI appearances and persistent acromegaly

Twenty-six patients with acromegaly had active disease (cases 5–30) despite previous treatment(s) (Table 1). The majority of patients had undergone single TSS (n=18). Two patients had undergone repeat TSS (cases 15 & 16), one of whom (case 16) had also received post-operative RT. Two patients (cases 26 & 29) had undergone single TSS followed by RT. Another patient (case 30) had undergone TSS, conventional RT and stereotactic radiosurgery sequentially, with continuing poor control necessitating maximum dose of pegvisomant. Three further patients (cases 17, 18, 19) had never been offered surgery due to the absence of a clear surgical target on MRI, which showed a large, partially empty sella (Table 1). Several patients were receiving adjunctive medical therapy (depot SSA in 17; cabergoline in one), which was discontinued prior to Met-PET/MRI (see above).

In 25 cases (96%), Met-PET/MRI revealed tracer uptake at sites that were clearly visualised to be separate from the normal pituitary gland (Table 1 and Figs. 3-7). Some, but not all of these sites had been independently identified as suspicious for residual adenoma on MRI, but with the caveat that the reporting radiologists (and referring pituitary multidisciplinary teams) were unable to definitively distinguish them from post-treatment changes. In one patient (case 8), Met-PET/MRI did not show any tracer uptake at a site of suspected recurrence (5mm area adjacent to the left cavernous sinus).

However, it transpired that this patient had received a 90mg depot injection of Lanreotide Autogel® (ATG) just five weeks prior to being scanned, which may have suppressed ^{11}C-Methionine uptake by the tumour.

Based on the Met-PET/MRI findings, 14 patients were referred for first or repeat TSS (Table 1). In all 14 cases tumour was localised intra-operatively at the sites previously identified as abnormal on Met-PET/MRI, and histological analysis confirmed GH-secreting pituitary adenoma in all but two patients; both of the latter, however, remain in full remission at one and two years' follow up respectively off all treatment (case 7 and case 19). Post-operative endocrine testing (6-12 weeks after TSS and a minimum of 12 weeks after discontinuing medical therapy) showed a marked improvement in disease control in seven patients (with IGF-1 <2.0 ×ULN in six subjects), and complete biochemical remission in the other seven cases (Table 1). Reassuringly, only one patient developed new pituitary hormone deficits following Met-PET/MRI guided surgery (LH, FSH, TSH in subject 5). The only other patient to acquire a new hormone deficit (ACTH) following TSS was case 8 (the single subject with a negative Met-PET/MRI) (Table 1).

One patient underwent stereotactic radiosurgery (case 28) and achieved biochemical control at one year post-treatment; he is now being considered for withdrawal of medical therapy. Two patients (cases 21 & 22), in whom Met-PET/MRI demonstrated clear cavernous sinus invasion, received adjunctive fractionated RT with subsequent normalisation of GH and IGF-1 off all medical therapy by 24 and 48 months respectively. Five patients (cases 23-27) were treated with SSA after rejecting alternative treatment options (Table 1). Three patients are currently awaiting further surgery or stereotactic radiosurgery.

Discussion

In an important subgroup of patients with acromegaly, post-treatment MRI (and/or CT) is unable to reliably identify the site(s) of residual/recurrent pituitary adenoma or distinguish suspected adenoma from post-therapy change (e.g. sella remodelling due to scar tissue). In this setting, adjunctive medical therapy (e.g. SSA, dopamine agonist, pegvisomant) or fractionated radiotherapy are often preferred because of the lack of a clear target for (repeat) TSS or stereotactic radiosurgery (SRS). While good disease control can be achieved in the majority of patients with medical therapy and/or conventional radiotherapy, they are associated with significant long-term cost (e.g. SSA, pegvisomant) or potential adverse effects (e.g. hypopituitarism following radiotherapy). Here, we have shown in the largest cohort of acromegaly patients studied to date that Met-PET/MRI can provide additional data (Figs. 3–7) to help inform management in such cases, and may facilitate further targeted treatment with a high probability of achieving a significant improvement in, or complete, disease control. Met-PET/MRI can also exclude suspected residual tumour following successful surgery (Figs. 1 and 2).

A potential role for functional imaging with PET in pituitary disease has previously been suggested by several groups (2, 3, 8-11, 19). Proposed indications include detection of microadenomas where MRI is either negative or inconclusive (e.g. in up to 40% of Cushing's disease) (10, 19), discrimination between post-operative changes and residual active adenoma (in non-functioning and functioning tumours) (3, 9, 11), and to evaluate the effects of treatment (e.g. radiotherapy, medical therapy) (2, 8, 20). Although FDG-PET has shown utility in some patients, its limited sensitivity (especially for detecting microadenomas) coupled with high background uptake by normal brain have prevented its adoption into routine clinical practice. In contrast, ^{11}C-methionine shows considerably lower brain uptake (producing a much more favourable target:background ratio), with several studies also reporting increased sensitivity compared with FDG-PET (10, 11). Estimation of tumour metabolism through measurement of the maximum standard(ised) uptake value (SUV_{max}), and comparison to background cerebellar uptake, may help to confirm non-physiological sella uptake (a ratio >2 has been proposed as exceeding that seen in normal pituitary tissue) (2), although ratios <2 may be seen in some tumour subtypes (e.g. corticotroph microadenomas) or when there is low volume residual disease,

making this an unreliable means of confirming or refuting the presence of residual functioning tumour (9, 10).

Early PET studies were limited by a lack of spatial resolution, and even modern PET-CT cannot match the anatomical definition offered by MRI (21). In pituitary disease this presents significant challenges, for example when trying to locate a small (<5mm) microadenoma within an otherwise normal gland, or determine whether laterally-situated tumour is simply abutting or invading (and therefore potentially unresectable) the adjacent cavernous sinus (11). In recognition of this, a small number of studies have been performed in which PET-CT images have been co-registered with contemporaneous fine slice MRI (thereby combining the sensitivity of PET-CT with the anatomical resolution of MRI), with initial reports suggesting significant benefits for tumour localisation (9, 10, 19). If confirmed, these findings provide strong support for future studies using PET-MR.

To date, only a relatively small number of patients with acromegaly have been included in studies of Met-PET, but with generally positive findings. For example, Tang and colleagues studied four patients with acromegaly in a group of 33 patients with biochemical or radiological evidence of pituitary adenoma recurrence following surgery (3). In 14 of these patients (three of whom had persisting acromegaly), Met-PET detected residual tumour which was not visible on MRI. This information was used to guide stereotactic radiosurgery in 9 patients, including one of those with acromegaly (3). More recently, Rodriguez-Barcelo et al studied 17 patients with newly diagnosed or surgically treated acromegaly using co-registered PET-CT and MRI. They reported 86% sensitivity and 86% specificity for detecting recurrence following surgery. However, importantly only one patient proceeded to PET guided treatment (SRS), and no outcome data were provided to confirm the accuracy of the imaging findings (9). Feng and colleagues, comparing FDG-PET-CT and Met-PET in 43 patients with secretory pituitary adenomas, including 16 patients with acromegaly, concluded that while FDG-PET showed high specificity, Met-PET demonstrated greater sensitivity (11). Interestingly, all patients in their cohort had visible tumours on MRI.

Our study significantly extends these earlier findings, reporting the outcomes of Met-PET/MRI in 30 UK patients in whom specialist pituitary multidisciplinary teams had concluded that post-treatment MRI appearances were indeterminate. We therefore deliberately focused on cases in whom management decisions could benefit from additional information regarding the location of residual tumour [i.e. those who might be considered for further surgery, SRS or focused fractionated radiotherapy (i.e. confined to site of suspected tumour remnant only)]. We have also provided detailed surgical, pathological and post-operative data for each case, thus correlating Met-PET/MRI findings with key clinical outcomes.

Importantly, in four patients with suspected residual tumour on post-operative MRI, but no clinical or biochemical evidence of active disease, Met-PET/MRI demonstrated no abnormal tracer uptake (Figs. 1 and 2). Such findings may explain the apparent discrepancies noted by other workers in post-surgical acromegaly (22). In contrast, in 25 of 26 patients with persistent disease following primary therapy, Met-PET/MRI identified one or more foci of abnormal tracer uptake either confirming suspicious areas seen on MRI or revealing previously unsuspected sites of residual disease (Table 1) (Figs. 3–7). In all 25 patients the findings of Met-PET/MRI were used to inform decision-making by a specialist pituitary multidisciplinary team with respect to adjunctive therapy. In 15 patients repeat (n=12) or first (n=3) TSS were advised, and in the 14 patients operated to date, all had intraoperative confirmation of residual tumour at the sites suspected on Met-PET/MRI. Although two patients had negative histology, both remain in remission after TSS. All patients experienced a significant improvement in disease control, with six achieving IGF-1 $<2.0\times$ULN and seven full biochemical remission. Interestingly, in the three patients considered to have a predominantly empty sella on initial MRI, such that surgery was not considered advisable, Met-PET/MRI identified clear foci of microscopic disease (subsequently confirmed at surgery to be adherent to a thin layer of residual normal pituitary tissue) (Fig. 6). Two of these patients were able to discontinue medical therapy completely following surgery, while the third had an 85% reduction in GH levels. For other patients, Met-PET/MRI confirmed the suspicion of significant parasellar disease and led to recommendations to continue adjunctive medical therapy or consider fractionated RT or SRS (Table 1).

In one patient (case 29) Met-PET/MRI offered an explanation for the failure of previous SRS to achieve complete disease control, identifying foci of residual functioning adenoma that were outside the SRS treatment field (Fig. 7).

We believe our findings therefore provide additional evidence to support a role for Met-PET/MRI in selected cases of acromegaly where there is evidence of residual disease activity following primary therapy, but in whom post-treatment MRI is inconclusive. Specifically, we have identified three potential indications:

i. To distinguish between residual functioning tumour and post-treatment remodelling
ii. To delineate sites of residual adenoma that are potentially amenable to (further) surgery or targeted radiotherapy in patients with persistent disease following primary therapy, but indeterminate MRI findings
iii. To confirm sites of residual functioning tumour following failed RT or SRS

Met-PET/MRI has one major drawback - due to the short half-life of ^{11}C-methionine (~20 min), scanning can only be performed in PET centres with an adjacent cyclotron. This inevitably means that some patients will need to travel significant distances to be imaged. However, it can be argued that concentrating expertise in only a small number of centres is also potentially desirable, especially for a technique that is only likely to find use in a subgroup of patients. In addition, our observations in case 8 are consistent with previous reports that medical treatment which specifically suppresses hormone synthesis may result in a false negative scan. Accordingly, we would agree with previous recommendations to discontinue depot SSA therapy 12 weeks, and dopamine agonist therapy 4 weeks, prior to functional imaging with ^{11}C-methionine PET.

Conclusions

Met-PET/MRI represents an important opportunity for personalising management (23) in selected patients with acromegaly. We have shown that accurate localisation of residual tumour can facilitate targeted therapy to increase the rate of clinical and biochemical remission, while preserving normal pituitary function, and potentially sparing expensive long-term medical treatment or the adverse effects of RT.

Acknowledgements

We thank clinicians who have referred patients to our centre for further investigation. We also thank the WBIC Radiopharmaceutical Unit team. OK, ASP, NB, JDP and MG are supported by the NIHR Cambridge Biomedical Research Centre. JDP has received support by an NIHR Senior Investigator award and NIHR brain injury HTC.

Disclosure

OK, ASP, AKA and MG are supported by an unconditional award from Ipsen Ltd.

This research did not receive any specific grant from any funding agency in the public, commercial or not-for-profit sector.

References

1. Nomikos P, Buchfelder M, Fahlbusch R. The outcome of surgery in 668 patients with acromegaly using current criteria of biochemical 'cure'. *European Journal of Endocrinology.* 2005 **152** 379–87.
2. Bergström M, Muhr C, Lundberg PO, Långström B. PET as a tool in the clinical evaluation of pituitary adenomas. *Journal of Nuclear Medicine* 1991 **32** 610–5.
3. Tang BN, Levivier M, Heureux M, Wikler D, Massager N, Devriendt D, David P, Dumarey N, Corvilain B, Goldman S. 11C-methionine PET for the diagnosis and management of recurrent pituitary adenomas. *European Journal of Nuclear Medicine and Molecular Imaging* 2006 **33** 169–78.
4. Littley MD, Shalet SM, Beardwell CG, Ahmed SR, Applegate G, Sutton ML. Hypopituitarism following external radiotherapy for pituitary tumours in adults. *Quarterly Journal of Medicine* 1989 **70** 145–60.
5. Minniti G, Traish D, Ashley S, Gonsalves A, Brada M. Risk of second brain tumor after conservative surgery and radiotherapy for pituitary adenoma: update after an additional 10 years. *Journal of Clinical Endocrinology and Metabolism* 2005 **90** 800–4.
6. Sattler MG, Vroomen PC, Sluiter WJ, Schers HJ, van den Berg G, Langendijk JA, Wolffenbuttel BH, van den Bergh AC, van Beek AP. The incidence of second tumours and mortality in pituitary adenoma patients treated with postoperative radiotherapy versus surgery alone. *Radiotherapy and Oncology* 2012 **104** 125–30.
7. Sattler MG, Vroomen PC, Sluiter WJ, Schers HJ, van den Berg G, Langendijk JA, Wolffenbuttel BH, van den Bergh AC, van Beek AP. Incidence, causative mechanisms, and anatomic localization of stroke in pituitary adenoma patients treated with postoperative radiation therapy versus surgery alone. *International Journal of Radation Oncology, Biology, Physics* 2013 **87** 53–9.
8. Muhr C. Positron emission tomography in acromegaly and other pituitary adenoma patients. *Neuroendocrinology* 2006 **83** 205–10.

9. Rodriguez-Barcelo S, Gutierrez-Cardo A, Dominguez-Paez M, Medina-Imbroda J, Romero-Moreno L, Arraez-Sanchez M.Clinical usefulness of coregistered 11C-methionine positron emission tomography/3-T magnetic resonance imaging at the follow-up of acromegaly. *World Neurosurgery* 2014 **82** 468–73.

10. Ikeda H, Abe T, Watanabe K. Usefulness of composite methionine-positron emission tomography/3.0-tesla magnetic resonance imaging to detect the localization and extent of early-stage Cushing adenoma. *Journal of Neurosurgery* 2010 **112** 750–5.

11. Feng Z, He D, Mao Z, Wang Z, Zhu Y, Zhang X, Wang H. Utility of 11C-Methionine and 18F-FDG PET/CT in Patients With Functioning Pituitary Adenomas. *Clinical Nuclear Medicine* 2016 **41** e130–4.

12. Tomura N, Saginoya T, Mizuno Y, Goto H. Accumulation of 11C-methionine in the normal pituitary gland on 11C-methionine PET. *Acta Radiologica* 2016 doi:10.1177/0284185116651005

13. Giustina A, Chanson P, Bronstein MD, Klibanski A, Lamberts S, Casanueva FF, Trainer P, Ghigo E, Ho K, Melmed S; Acromegaly Consensus Group. A consensus on criteria for cure of acromegaly. *Journal of Clinical Endocrinology and Metabolism* 2010 **95** 3141–8.

14. Katznelson L, Laws ER Jr, Melmed S, Molitch ME, Murad MH, Utz A, Wass JA; Endocrine Society. Acromegaly: an endocrine society clinical practice guideline. *Journal of Clinical Endocrinology and Metabolism* 2014 **99** 3933–51.

15. Pascali C. Bogni A, Iwata R, Bombardieri E. High efficiency preparation of L-[S-methyl-11C]methionine by on-column [11C]methylation on C18 Sep-Pak. *Journal of Labelled Compounds and Radiopharmaceuticals* 1999 **42** 715–724.

16. Mitterhauser M, Wadsak W, Krcal A, Kletter K. New aspects on the preparation of [11C]Methionine--a simple and fast online approach without preparative HPLC. *Applied Radiation and Isotopes* 2005 **62** 441–5.

17. Gómez V, Gispert JD, Amador V, Llop J. New method for routine production of L-[methyl-11C]methionine:in loop synthesis. *Journal of Labelled Compounds and Radiopharmaceuticals* 2008 **51** 83–86.

18. Knosp E, Steiner E, Kitz K, Matula C. Pituitary adenomas with invasion of the cavernous sinus space: a magnetic resonance imaging classification compared with surgical findings. *Neurosurgery* 1993 **33** 610–7; discussion 617–8.

19. Koulouri O, Steuwe A, Gillett D, Hoole AC, Powlson AS, Donnelly NA, Burnet NG, Antoun NM, Cheow H, Mannion RJ, Pickard JD, Gurnell M. A role for 11C-methionine PET imaging in ACTH-dependent Cushing's syndrome. *European Journal of Endocrinology* 2015 **173** M107–20.

20. van den Bergh AC, Pruim J, Links TP, van der Vliet AM, Sluiter W, Wolffenbuttel BH, Langendijk JA, Hoving EW, Dullaart RP. Tyrosine positron emission tomography and protein synthesis rate in pituitary adenoma: Different effects of surgery and radiation therapy. *Radiotheapy and Oncology* 2011 **98** 213–216.

21. Chittiboina P, Montgomery BK, Millo C, Herscovitch P, Lonser RR. High-resolution(18)F-fluorodeoxyglucose positron emission tomography and magnetic resonance imaging for pituitary adenoma detection in Cushing disease. *Journal of Neurosurgery* 2015 **122** 791–7.

22. Jane JA, Starke RM, Elzoghby MA, Reames DL, Payne SC, Thorner MO, Marshall JC, Laws ER Jr, Vance ML., Endoscopic transsphenoidal surgery for acromegaly: remission using modern criteria, complications, and predictors of outcome. *Journal of Clinical Endocrinology and Metabolism* 2011 **96** 2732–40.

23. Melmed, S. Pituitary Medicine From Discovery to Patient-Focused Outcomes. *Journal of Clinical Endocrinology and Metabolism* 2016 **101** 769–77.

Figure legends

Figure 1: Case 1 (acromegaly in remission post-TSS). Post-operative MRI suggests a significant right-sided tumour remnant (white arrows), with normal gland (contrast enhanced, yellow arrow) displaced superiorly to the left; but Met-PET/MRI demonstrates tracer uptake only at the site of the normal gland, and confirms no residual functioning tumour at the site of the suspected remnant reported on routine clinical MRI.

Key: Met-PET, ^{11}C-methionine PET-CT; Met-PET/MRI, co-registered ^{11}C-methionine PET-CT and MRI; SE, spin echo; SPGR, spoiled gradient recalled; T1W, T1-weighted; TSS, transsphenoidal surgery.

Figure 2: Case 2 (acromegaly in remission post-TSS). Post-operative MRI suggests a possible tumour remnant (white arrows), inferior to the normal gland (contrast enhanced, yellow arrows). Met-PET/MRI demonstrates tracer uptake only at the site of the normal gland, and confirms no residual functioning tumour at the site of the suspected remnant

Key: Met-PET, ^{11}C-methionine PET-CT; Met-PET/MRI, coregistered ^{11}C-methionine PET-CT and MRI; SE, spin echo; SPGR, spoiled gradient recalled; T1W, T1-weighted; TSS, transsphenoidal surgery.

Figure 3: Case 5 (persistent active acromegaly post-first TSS). Post-operative MRI suggests a possible sella remnant [white arrows inferior to normal gland (yellow arrows)]; Met-PET/MRI reveals tracer uptake (white arrows) in the sella and adjacent to the left internal carotid artery where the greatest intensity is observed (Met-PET axial image, white arrow).

Key: Met-PET, ^{11}C-methionine PET-CT; Met-PET/MRI, co-registered ^{11}C-methionine PET-CT and MRI; SE, spin echo; SPGR, spoiled gradient recalled; T1W, T1-weighted; TSS, transsphenoidal surgery.

Figure 4: Case 11 (persistent active acromegaly post-first TSS). Post-operative MRI shows a thin rind of enhancing tissue lining the floor of the sella (yellow area) with a hypointense area adjacent to / extending into the left cavernous sinus (white arrows). Met-PET/MRI reveals tracer uptake predominantly in the left side of the sella adjacent to the cavernous sinus (white arrows), with greatest intensity seen at the posterior aspect (Met-PET axial image, white arrow).

Key: Met-PET, 11C-methionine PET-CT; Met-PET/MRI, coregistered 11C-methionine PET-CT and MRI; SE, spin echo; SPGR, spoiled gradient recalled; T1W, T1-weighted; TSS, transsphenoidal surgery.

Figure 5: Case 16 (persistent active acromegaly despite TSS×2 and fractionated RT). MRI shows a suspicious area on the right side of the sella with possible cavernous sinus extension (white arrows). Met-PET/MRI confirms tracer uptake in this area without evidence of cavernous sinus invasion. The position of presumed residual normal pituitary tissue is also shown (yellow arrow).

Key: Met-PET, ^{11}C-methionine PET-CT; Met-PET/MRI, co-registered ^{11}C-methionine PET-CT and MRI; RT, fractionated radiotherapy; SE, spin echo; SPGR, spoiled gradient recalled; T1W, T1-weighted; TSS, transsphenoidal surgery.

Figure 6: Case 17 (persistent active acromegaly despite maximum dose pegvisomant). MRI shows an enlarged, partially empty sella with no convincing 'surgical target'. Met-PET reveals foci of increased tracer uptake throughout the sella (white arrows) with maximum left-sided intensity. Met-PET/MRI localizes the sites of increased tracer uptake in the pituitary fossa with maximum intensity on the left.

Key: Met-PET, ^{11}C-methionine PET; Met-PET/MRI, co-registered ^{11}C-methionine PET-CT and MRI; SE, spin echo; SPGR, spoiled gradient recalled; T1W, T1-weighted; TSS, transsphenoidal surgery.

Figure 7: Case 29 (persistent active acromegaly post-first TSS and RT). Post-operative MRI shows a thin rind of poorly enhancing tissue within the floor of the sella [white arrow, coronal (1) image] and a possible second discrete hypointense area adjacent to the left cavernous sinus [white

arrow, coronal (2) image]. The pituitary stalk is displaced to the right (yellow arrow). Met-PET/MRI reveals tracer uptake at both sites of suspected residual tumour (white arrows), with greatest intensity seen in the tissue lining the floor of the sella centrally (Met-PET axial image, dashed white arrow).

Key: Met-PET, ^{11}C-methionine PET-CT; Met-PET/MRI, co-registered ^{11}C-methionine PET-CT and MRI; RT, fractionated radiotherapy; SE, spin echo; SPGR, spoiled gradient recalled; T1W, T1-weighted; TSS, transsphenoidal surgery.

Table 1 Patient demographics and biochemical and radiological findings at presentation and following primary and adjunctive treatment.

Case	Age/ Sex	MRI findings at initial presentation	Previous treatment	GH and IGF-1 levels following previous treatment			MRI findings following previous treatment	Met-PET/MRI findings	Adjunctive therapy	GH and IGF-1 levels following adjunctive therapy			New pituitary deficits following adjunctive therapy
				OGTT GH nadir (mcg/L)	GH (mcg/L)	IGF-1 (×ULN)				OGTT GH nadir (mcg/L)	GH (mcg/L)	IGF-1 (×ULN)	
1	34/F	21mm macro; SSE; right CSE	TSS	0.34	0.77[a]	0.74	Right sella remnant ± right CSE	No tracer uptake at site of suspected remnant	Not required	-	-	-	-
2	47/M	17mm macro; minor SSE; SpE	TSS	0.62	1.23[a]	0.83	Central sella/SpE remnant inferior to normal gland	No tracer uptake at site of suspected remnant	Not required	-	-	-	-
3	25/M	12.5mm macro; SSE	TSS	<0.05	0.15[a]	0.97	? left sella remnant	No tracer uptake at site of suspected remnant	Not required	-	-	-	-
4	57/F	11mm macro; left CSE	TSS	0.20	0.38[b]	0.70	Left sella remnant	No tracer uptake at site of suspected remnant	Not required	-	-	-	-
5	30/F	22mm macro; SSE; left CSE; SpE	TSS	10.00	31.2[a]	3.58	? discrete central sella and left CS remnants	Tracer uptake in suspected sella and CS remnants	Repeat TSS	1.80	2.30[a]	1.35	LH, FSH, TSH
6	45/F	19mm macro; left CSE	TSS	2.00	4.00[a]	2.75	Small left sella remnant	Tracer uptake in discrete right and left sella remnants	Repeat TSS	0.32	0.45[a]	0.64	None
7	53/F	15mm macro	TSS	1.00	4.20[a]	2.63	Central sella remnant inferior to normal gland	Tracer uptake in suspected sella remnant	Repeat TSS	0.07	0.60[a]	0.56	None
8	58/M	7mm micro	TSS	0.88	1.50[a]	2.26	Small left sella remnant	No tracer uptake at site of suspected remnant*	Repeat TSS	0.50	0.80[a]	1.50	ACTH
9	24/F	26mm macro; left CSE	TSS	12.6	10.83[a]	4.29	Central/left sella remnant; ? left CSE	Majority of tracer uptake within sella remnant; small amount of left CS uptake	Repeat TSS	2.70	3.30[a]	1.68	None
10	49/F	16mm macro	TSS	4.19	6.4[b]	2.07	? discrete right and left sella remnants	Tracer uptake in both suspected remnants	Repeat TSS	0.58	0.93	0.72	None
11	36/M	27.5mm macro; SSE; left CSE	TSS	4.19	na	3.5	left sella remnant with probable left CSE	Majority of tracer uptake within sella remnant; small amount of left CS uptake	Repeat TSS	2.8	na	2.18	None
12	56/M	18.5mm macro; right CSE	TSS	1.6	na	1.32	? discrete right (±CSE) and left sella remnants	Tracer uptake in both suspected remnants; no CS uptake	Repeat TSS	<0.05	0.47	0.55	None
13	52/M	40mm macro; SSE; left CSE; SpE	TSS	2.93	3.06[b]	2.69	? sella and sphenoid sinus remnants	Tracer uptake in right sella and part of sphenoid sinus remnant	Repeat TSS	0.89	na	1.53	None

14	54/M	11mm macro	TSS	na	1.76[a]	2.35	right sella remnant	Tracer uptake in right sella remnant	Repeat TSS	0.84	1.30[b]	1.87	None
15	42/M	17mm macro	TSSx2	2.51	2.51[b]	2.24	? right sella remnant; ? right CSE	Tracer uptake in suspected remnant, no CS uptake	Repeat TSS	1.28	0.71[b]	1.18	None
16	63/M	27 mm macro; SSE; right CSE	TSSx2; Fractionated RT	3.55	3.08	1.94	right sella remnant; ? right CSE	Tracer uptake only within right sella remnant; no CSE	Repeat TSS	0.54	1.90	0.79	None
17	68/F	Enlarged partial empty sella	Pegvisomant 30mg/day	-	-	3.40	Thin rind of tissue lining an enlarged sella	Several foci of tracer uptake - maximum left sella	First TSS	0.63	0.80	0.67	None
18	41/M	Enlarged partial empty sella	Cabergoline 3mg/week	-	21.5[b]	3.02	Thick rind of tissue lining an enlarged sella	Tracer uptake lining whole sella – maximum on left	First TSS	3.30	3.70[b]	1.88	None
19	51/M	Enlarged partial empty sella	ATG 120mg 4-weekly	-	1.30[b]	1.40	Thin rind of tissue lining an enlarged sella	Tracer uptake lining sella – focal area of maximal uptake on left	First TSS	<0.1	<0.1	0.48	None
20	51/F	25 mm macro; SSE	TSS	na	20.50	2.3	Thin rind of tissue lining sella	Tracer uptake throughout sella – maximum on left	Awaiting repeat TSS	na	na	na	-
21	26/F	26 mm macro; SSE; right CSE	TSS	1.40	4.65[a]	1.63	? right sella remnant; extensive right CSE	Tracer uptake only within right parasellar/CS tumour	Fractionated RT	-	0.64[a]	0.46	None
22	41/F	40 mm macro; SSE, right CSE	TSS	9.7	7.04[a]	3.04	Inferior sella remnant with right CSE	Tracer uptake in right CSE; some sella uptake	Fractionated RT	-	1.55[b]	0.43	ACTH
23	43/F	28.5 mm macro; left CSE; SpE	TSS	1.21	1.30[a]	1.30	? left sella remnant; clear left CS remnant	Tracer uptake in left CSE; some adjacent sella uptake	ATG 90mg 4-weekly	-	0.59[a]	0.77	-
24	75/F	Macro[$]	TSS	1.9	2.50[b]	1.65	? discrete right and left sella remnants	Tracer uptake in both suspected sella remnants	ATG 120mg 4-weekly	-	na	0.88	-
25	51/F	18mm macro; CSE; SpE	TSS	na	na	1.15	? left sella remnant; ? CSE	No sella uptake; tracer uptake in left CSE	ATG 120mg 4-weekly	-	0.50[b]	0.72	-
26	55/M	Macro[$]	TSS; Fractionated RT	2.25	2.78	2.49	Thin rind of tissue lining the sella	Tracer uptake in right sella + small focus left of centre	ATG 120mg 4-weekly	-	na	na	-
27	60/F	Macro[$]	TSS	na	1.40	2.19	? right cavernous sinus remnant	Tracer uptake in right CSE and discrete focus in left sella	ATG 120mg 4-weekly	-	0.83[a]	1.5	-
28	52/M	14.5mm macro; No SSE; right CSE	TSS	6.6	na	4.5	? right sella remnant	Tracer uptake in right sella remnant	SRS + ATG 120mg 4-weekly	-	0.9[b]	1.2	na
29	55/M	15 mm macro; ? left CSE	TSS; Fractionated RT	na	na	2.6	? left sella remnant	Discrete foci of tracer uptake in mid-sella and left sella regions	Awaiting SRS	na	na	na	na
30	38/F	Macro; SSE	TSS; Fractionated RT; SRS	na	49	1.83	Enlarged, partially empty sella, no discrete residual adenoma	Foci of tracer uptake in posterior right > left sella	Awaiting SRS	na	na	na	na

Key: ATG, lanreotide Autogel®; CS, cavernous sinus; CSE, cavernous sinus extension; macro, macroadenoma; micro, microadenoma; na, not available; OGTT, 75 g oral glucose tolerance test; RT, radiotherapy; SRS, stereotactic radiosurgery; SSE, suprasellar extension; SpE, sphenoid sinus extension; TSS, transsphenoidal surgery; *Patient scanned while receiving ATG therapy (90 mg four weekly); [a] denotes mean GH value from 5-point day curve; [b] denotes single random GH level; - denotes measurement not indicated; [$]dimensions unknown as presenting MRI unavailable.

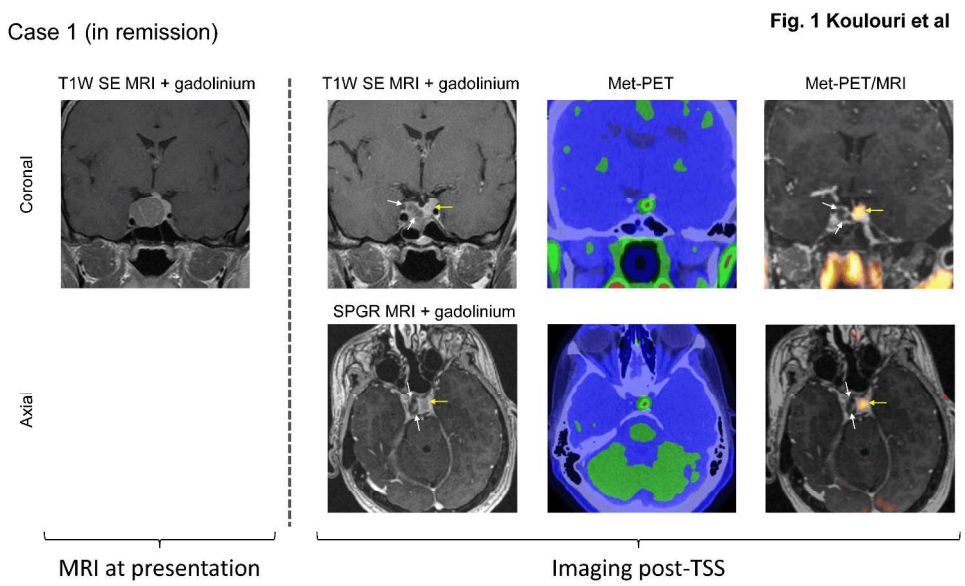

Figure 1: Case 1 (acromegaly in remission post-TSS). Post-operative MRI suggests a significant right-sided tumour remnant (white arrows), with normal gland (contrast enhanced, yellow arrow) displaced superiorly to the left; but Met-PET/MRI demonstrates tracer uptake only at the site of the normal gland, and confirms no residual functioning tumour at the site of the suspected remnant reported on routine clinical MRI.
Key: Met-PET, 11 C-methionine PET-CT; Met-PET/MRI, co-registered 11 C-methionine PET-CT and MRI; SE, spin echo; SPGR, spoiled gradient recalled; T1W, T1-weighted; TSS, transsphenoidal surgery.
Figure 1
254x148mm (300 x 300 DPI)

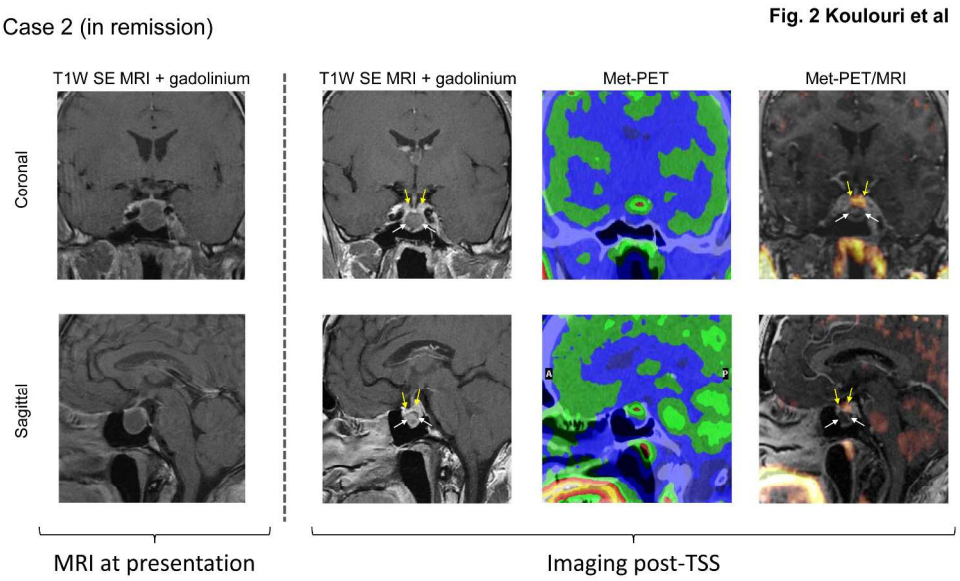

Figure 2: Case 2 (acromegaly in remission post-TSS). Post-operative MRI suggests a possible tumour remnant (white arrows), inferior to the normal gland (contrast enhanced, yellow arrows). Met-PET/MRI demonstrates tracer uptake only at the site of the normal gland, and confirms no residual functioning tumour at the site of the suspected remnant.
Key: Met-PET, 11 C-methionine PET-CT; Met-PET/MRI, coregistered 11 C-methionine PET-CT and MRI; SE, spin echo; SPGR, spoiled gradient recalled; T1W, T1-weighted; TSS, transsphenoidal surgery.
Figure 2
254x148mm (300 x 300 DPI)

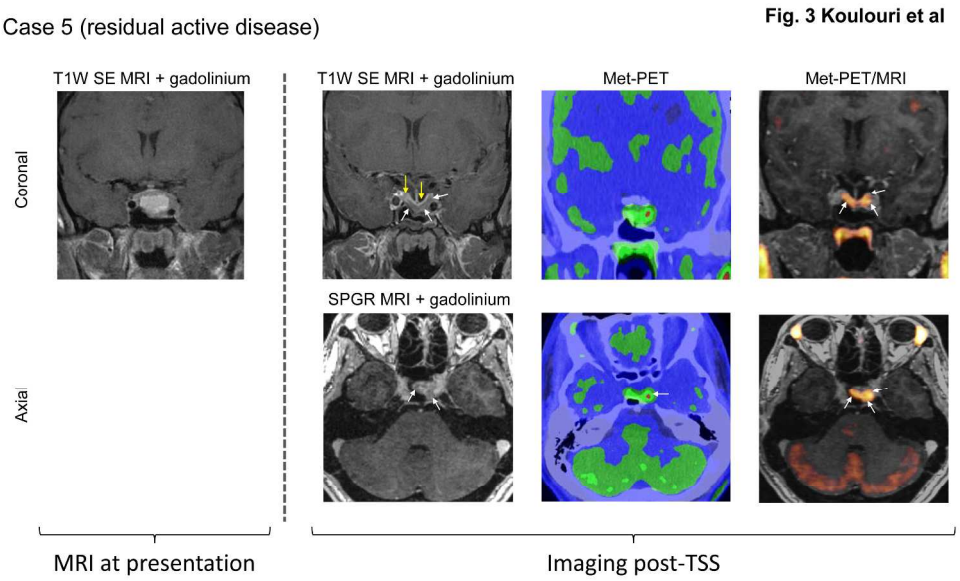

Figure 3: Case 5 (persistent active acromegaly post-first TSS). Post-operative MRI suggests a possible sella remnant [white arrows inferior to normal gland (yellow arrows)]; Met-PET/MRI reveals tracer uptake (white arrows) in the sella and adjacent to the left internal carotid artery where the greatest intensity is observed (Met-PET axial image, white arrow).

Key: Met-PET, 11 C-methionine PET-CT; Met-PET/MRI, co-registered 11 C-methionine PET-CT and MRI; SE, spin echo; SPGR, spoiled gradient recalled; T1W, T1-weighted; TSS, transsphenoidal surgery.

Figure 3

254x148mm (300 x 300 DPI)

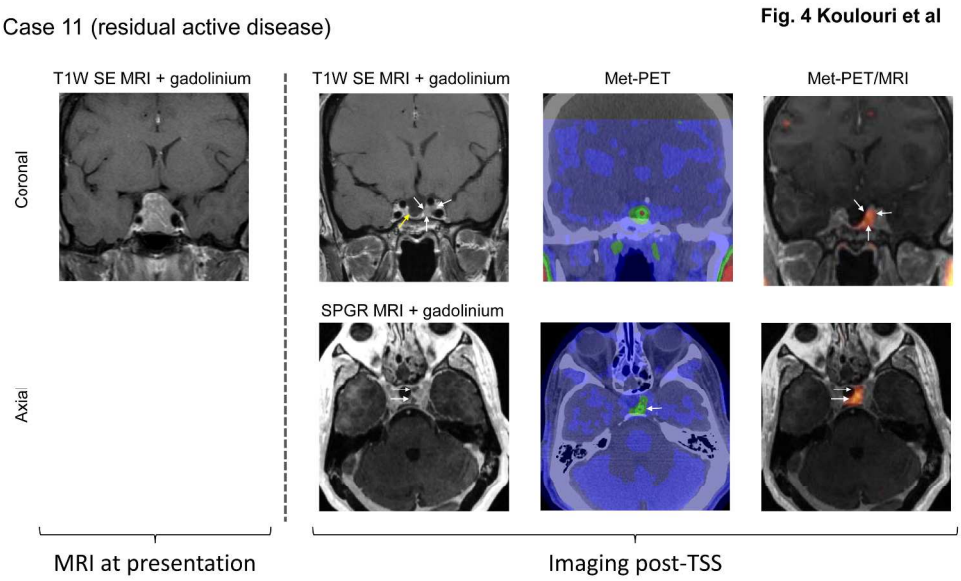

Figure 4: Case 11 (persistent active acromegaly post-first TSS). Post-operative MRI shows a thin rind of enhancing tissue lining the floor of the sella (yellow area) with a hypointense area adjacent to / extending into the left cavernous sinus (white arrows). Met-PET/MRI reveals tracer uptake predominantly in the left side of the sella adjacent to the cavernous sinus (white arrows), with greatest intensity seen at the posterior aspect (Met-PET axial image, white arrow).
Key: Met-PET, 11C-methionine PET-CT; Met-PET/MRI, coregistered 11C-methionine PET-CT and MRI; SE, spin echo; SPGR, spoiled gradient recalled; T1W, T1-weighted; TSS, transsphenoidal surgery.
Figure 4
253x148mm (300 x 300 DPI)

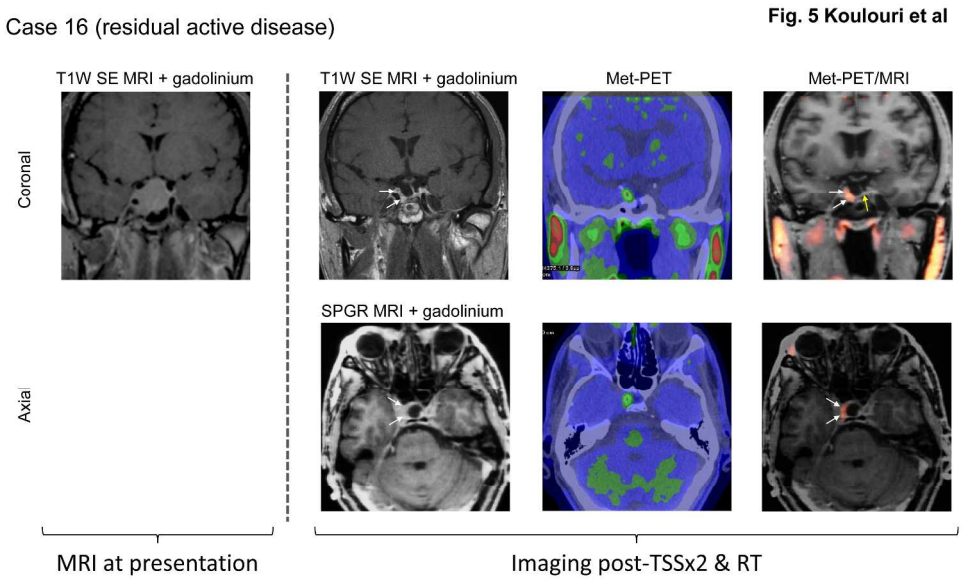

Figure 5: Case 16 (persistent active acromegaly despite TSS×2 and fractionated RT). MRI shows a suspicious area on the right side of the sella with possible cavernous sinus extension (white arrows). Met-PET/MRI confirms tracer uptake in this area without evidence of cavernous sinus invasion. The position of presumed residual normal pituitary tissue is also shown (yellow arrow).
Key: Met-PET, 11 C-methionine PET-CT; Met-PET/MRI, co-registered 11 C-methionine PET-CT and MRI; RT, fractionated radiotherapy; SE, spin echo; SPGR, spoiled gradient recalled; T1W, T1-weighted; TSS, transsphenoidal surgery.

Figure 5
254x148mm (300 x 300 DPI)

Fig. 6 Koulouri et al

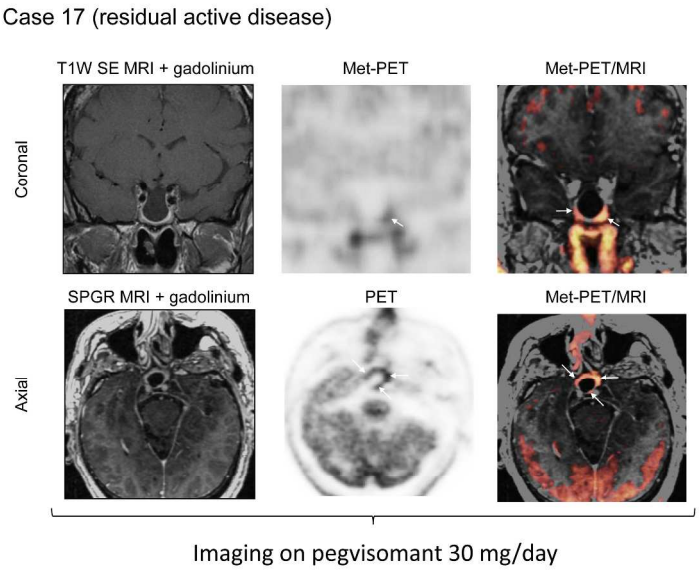

Figure 6: Case 17 (persistent active acromegaly despite maximum dose pegvisomant). MRI shows an enlarged, partially empty sella with no convincing 'surgical target'. Met-PET reveals foci of increased tracer uptake throughout the sella (white arrows) with maximum left-sided intensity. Met-PET/MRI localizes the sites of increased tracer uptake in the pituitary fossa with maximum intensity on the left. Key: Met-PET, 11 C-methionine PET; Met-PET/MRI, co-registered 11 C-methionine PET-CT and MRI; SE, spin echo; SPGR, spoiled gradient recalled; T1W, T1-weighted; TSS, transsphenoidal surgery.

Figure 6
254x148mm (300 x 300 DPI)

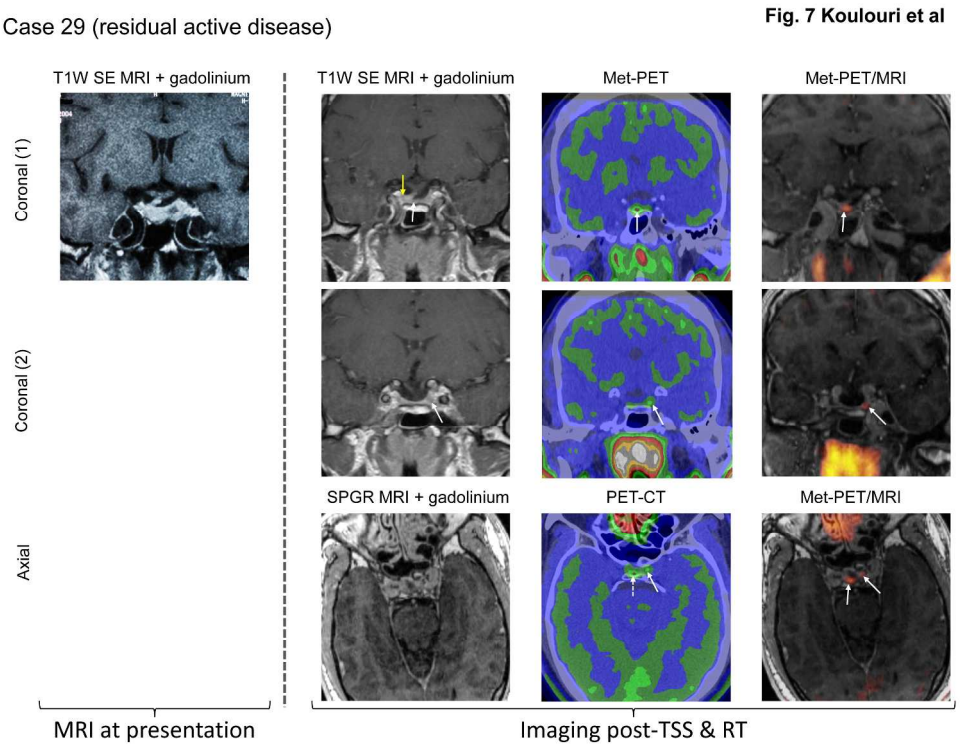

Figure 7: Case 29 (persistent active acromegaly post-first TSS and RT). Post-operative MRI shows a thin rind of poorly enhancing tissue within the floor of the sella [white arrow, coronal (1) image] and a possible second discrete hypointense area adjacent to the left cavernous sinus [white arrow, coronal (2) image]. The pituitary stalk is displaced to the right (yellow arrow). Met-PET/MRI reveals tracer uptake at both sites of suspected residual tumour (white arrows), with greatest intensity seen in the tissue lining the floor of the sella centrally (Met-PET axial image, dashed white arrow).
Key: Met-PET, 11 C-methionine PET-CT; Met-PET/MRI, co-registered 11 C-methionine PET-CT and MRI; RT, fractionated radiotherapy; SE, spin echo; SPGR, spoiled gradient recalled; T1W, T1-weighted; TSS, transsphenoidal surgery.
Figure 7
254x189mm (300 x 300 DPI)